JCI The Journal of Clinical Investigation

TLR4 signaling in effector CD4$^+$ T cells regulates TCR activation and experimental colitis in mice

José M. González-Navajas, … , Jongdae Lee, Eyal Raz

J Clin Invest. 2010;120(2):570-581. https://doi.org/10.1172/JCI40055.

Research Article **Immunology**

TLRs sense various microbial products. Their function has been best characterized in DCs and macrophages, where they act as important mediators of innate immunity. TLR4 is also expressed on CD4$^+$ T cells, but its physiological function on these cells remains unknown. Here, we have shown that TLR4 triggering on CD4$^+$ T cells affects their phenotype and their ability to provoke intestinal inflammation. In a model of spontaneous colitis, *Il10*$^{-/-}$*Tlr4*$^{-/-}$ mice displayed accelerated development of disease, with signs of overt colitis as early as 8 weeks of age, when compared with *Il10*$^{-/-}$ and *Il10*$^{-/-}$*Tlr9*$^{-/-}$ mice, which did not develop colitis by 8 months. Similar results were obtained in a second model of colitis in which transfer of naive *Il10*$^{-/-}$*Tlr4*$^{-/-}$ CD4$^+$ T cells into *Rag1*$^{-/-}$ recipients sufficient for both IL-10 and TLR4 induced more aggressive colitis than the transfer of naive *Il10*$^{-/-}$ CD4$^+$ T cells. Mechanistically, LPS stimulation of TLR4-bearing CD4$^+$ T cells inhibited ERK1/2 activation upon subsequent TCR stimulation via the induction of MAPK phosphatase 3 (MKP-3). Our data therefore reveal a tonic inhibitory role for TLR4 signaling on subsequent TCR-dependent CD4$^+$ T cell responses.

TLR4 signaling in effector CD4+ T cells regulates TCR activation and experimental colitis in mice

José M. González-Navajas, Sean Fine, Jason Law, Sandip K. Datta, Kim P. Nguyen, Mandy Yu, Maripat Corr, Kyoko Katakura, Lars Eckman, Jongdae Lee, and Eyal Raz

Department of Medicine, UCSD, La Jolla, California, USA.

TLRs sense various microbial products. Their function has been best characterized in DCs and macrophages, where they act as important mediators of innate immunity. TLR4 is also expressed on CD4+ T cells, but its physiological function on these cells remains unknown. Here, we have shown that TLR4 triggering on CD4+ T cells affects their phenotype and their ability to provoke intestinal inflammation. In a model of spontaneous colitis, *Il10*$^{-/-}$*Tlr4*$^{-/-}$ mice displayed accelerated development of disease, with signs of overt colitis as early as 8 weeks of age, when compared with *Il10*$^{-/-}$ and *Il10*$^{-/-}$*Tlr9*$^{-/-}$ mice, which did not develop colitis by 8 months. Similar results were obtained in a second model of colitis in which transfer of naive *Il10*$^{-/-}$*Tlr4*$^{-/-}$ CD4+ T cells into *Rag1*$^{-/-}$ recipients sufficient for both IL-10 and TLR4 induced more aggressive colitis than the transfer of naive *Il10*$^{-/-}$ CD4+ T cells. Mechanistically, LPS stimulation of TLR4-bearing CD4+ T cells inhibited ERK1/2 activation upon subsequent TCR stimulation via the induction of MAPK phosphatase 3 (MKP-3). Our data therefore reveal a tonic inhibitory role for TLR4 signaling on subsequent TCR-dependent CD4+ T cell responses.

Introduction

IL-10 is an antiinflammatory cytokine that regulates T cell proliferation and functions (1). *Il10*$^{-/-}$ mice develop spontaneous chronic enterocolitis with mucosal infiltration of lymphocytes, macrophages, and neutrophils (2) similarly to that observed in the mucosal tissues of humans with inflammatory bowel disease. The role of CD4+ T cells in colitis induction was confirmed in mice with a T cell–specific inactivation of the *Il10* gene (3), as these mice develop the same inflammatory phenotype observed in *Il10*$^{-/-}$ mice. The enterocolitis in the *Il10*$^{-/-}$ mice is largely attributed to dysfunctional Tregs. As in many other models of intestinal inflammation, the inflammatory response in the intestinal mucosa in this model of colitis depends on luminal bacteria and/or their inflammatory components (4, 5).

As TLRs recognize various signature microbial products (6), their activation pathways are central for the physiologic function of innate immunity. TLR-activated dendritic cells and macrophages produce proinflammatory cytokines and chemokines and express high levels of costimulatory molecules. Conversely, recent studies demonstrated that TLR signaling in intestinal epithelial cells inhibit inflammatory responses and support colonic homeostasis (7–9). The role of TLR expression on CD4+ T cell functionality has not been fully explored.

Since TLR and TCR share signaling pathways, e.g., MAPK, we hypothesized that TLR signaling in effector CD4+ T cells regulates their subsequent TCR activation. To address the role of TLR signaling in effector CD4+ T cells in colitis development, we used 2 models of intestinal inflammation: (a) colitis in *Il10*$^{-/-}$ mice and (b) colitis induced by adoptive transfer of naive CD4+ T cells into *Rag1*$^{-/-}$ recipients. Surprisingly, our results demonstrate that TLR4 expressed on effector CD4+ T cells plays an inhibitory role in the inflammatory profile of colitogenic T cells independent of TLR4 expression on innate immune cells.

Results

TLR4 deficiency aggravates IL-10–dependent colitis. Previous studies have identified the TLR expression profile of T cells (10). To investigate the potential role of these receptors in the development of colitis, we crossed *Tlr4*$^{-/-}$ or *Tlr9*$^{-/-}$ mice onto *Il10*$^{-/-}$ animals. We followed the animals for 2 months and then analyzed their colons for signs of inflammation. While *Il10*$^{-/-}$ and *Il10*$^{-/-}$*Tlr9*$^{-/-}$ mice did not develop obvious signs of intestinal inflammation at the age of 8 months, the *Il10*$^{-/-}$*Tlr4*$^{-/-}$ mice demonstrated overt colitis at the age of 8 weeks, i.e., thickening of the intestinal wall, diarrhea, enlarged spleen and mesenteric lymph nodes (MLNs) (Supplemental Figure 1; supplemental material available online with this article; doi:10.1172/JCI40055DS1). Histological analysis of the colon revealed that *Il10*$^{-/-}$*Tlr4*$^{-/-}$ mice developed severe inflammation, with a high degree of epithelial crypt hyperplasia (Figure 1A, transverse section) and marked infiltration of mononuclear cells in the colonic lamina propria (LP) (Figure 1B, cross section). Figure 1C displays quantitative morphometric analysis of these inflammatory parameters. In addition, we observed goblet cell depletion in the mucosal layers and an increase in epithelial cell proliferation (data not shown).

The colitis observed in *Il10*$^{-/-}$*Tlr4*$^{-/-}$ mice could result from altered microflora in these animals. To evaluate this possibility, we co-housed young *Il10*$^{-/-}$ with diseased *Il10*$^{-/-}$*Tlr4*$^{-/-}$ mice in the same cage to allow colonization of these 2 groups with the same microflora (11). Age- and sex-matched *Il10*$^{-/-}$ mice housed separately served as controls. *Il10*$^{-/-}$ mice, under each housing condition, were monitored weekly for signs of intestinal inflammation for an additional period of 6 weeks, and histological evaluation was performed at the end of this period. Under these conditions, the co-housed *Il10*$^{-/-}$ mice showed no difference in the develop-

Conflict of interest: The authors have declared that no conflict of interest exists.
Citation for this article: *J Clin Invest.* 2010;120(2):570–581. doi:10.1172/JCI40055.

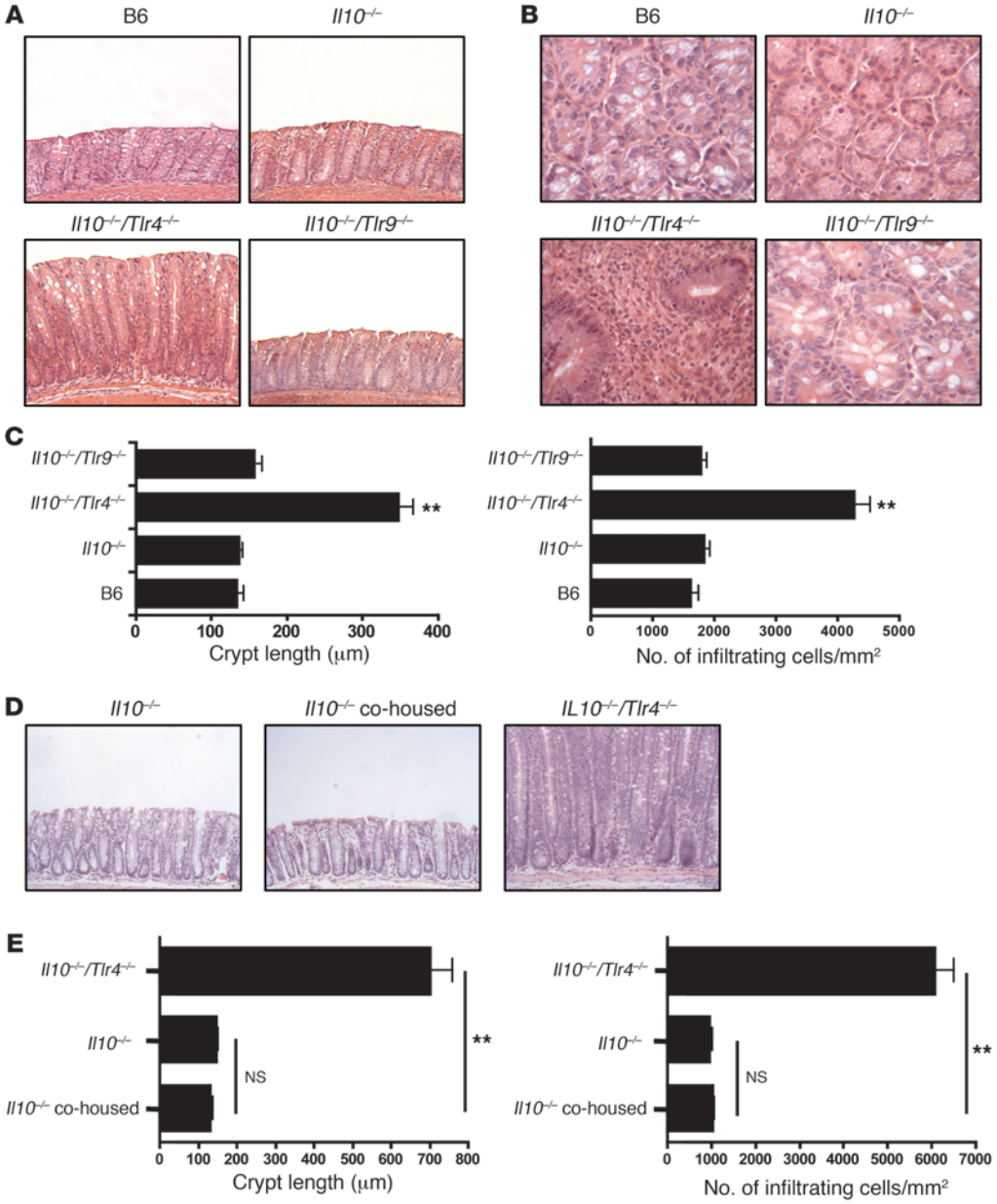

Figure 1
TLR4 deficiency aggravates colitis in *Il10*$^{-/-}$ mice. (**A**) Histological analysis of 8-week-old B6, *Il10*$^{-/-}$, *Il10*$^{-/-}$*Tlr9*$^{-/-}$, and *Il10*$^{-/-}$*Tlr4*$^{-/-}$ mice maintained under specific pathogen–free conditions showing increased epithelial crypt hyperplasia in *Il10*$^{-/-}$*Tlr4*$^{-/-}$ mice (original magnification, ×100). (**B**) Cross-sectional analysis of colons from the different mice showing greater cellular infiltration in the mice lacking TLR4 (original magnification, ×100). (**C**) Quantitative measurement of crypt length and cellular infiltration in the different groups of mice at 8 weeks of age. (**D**) Histological analysis of 4-week-old *Il10*$^{-/-}$ mice housed with or without 7- to 8-week-old *Il10*$^{-/-}$*Tlr4*$^{-/-}$ mice (original magnification, ×100). (**E**) Quantitative measurements of crypt length and cellular infiltration in co-housed animals. Data represent mean ± SEM of 3 different experiments. $^{**}P < 0.01$.

ment of intestinal inflammation compared with *Il10*$^{-/-}$ mice housed in separate cages (Figure 1D). Quantification of crypt length and cellular infiltration showed no difference between the colons of these 2 different groups (Figure 1E). Taken together, these data indicate that the lack of TLR4 accelerates the intestinal inflammation in the *Il10*$^{-/-}$ host.

Characterization of the inflammatory profile in Il10$^{-/-}$*Tlr4*$^{-/-}$ *mice*. To determine the inflammatory profile associated with colitis, we measured the mRNA levels of cytokines, chemokines, and cell markers in tissue homogenates obtained from the colons of each group of mice at 8 weeks of age. Consistent with the inflammatory phenotype, we found that *Il10*$^{-/-}$*Tlr4*$^{-/-}$ mice had increased transcript levels of inflammatory cytokines such as IL-6, IFN-γ, IL-1β, and IL-17A, as well as chemokines (keratinocyte chemoattractant [KC], macrophage inflammatory protein 1α [MIP1α], MIP1β, CCL22, and CXCL10). The mRNA levels of the cellular markers F4/80 (macrophages), MPO (neutrophils), and CD3d/CD4 (T cells) were also increased in the *Il10*$^{-/-}$*Tlr4*$^{-/-}$ mice as compared with the other tested groups (Table 1). To quantify the inflammatory mediators produced by the inflamed colons, we cultured ex vivo colonic explants (CEs) from *Il10*$^{-/-}$ and *Il10*$^{-/-}$*Tlr4*$^{-/-}$ mice. Supernatants from these cultures where then analyzed by ELISA. As shown in Figure 2A, the CEs from *Il10*$^{-/-}$*Tlr4*$^{-/-}$ mice released high amounts of IL-17A, IFN-γ, and TNF-α, whereas these cytokines were barely detectable in the supernatants harvested from the *Il10*$^{-/-}$ CEs. To further evaluate the inflammatory phenotype in the colons of these mice, intraepithelial lymphocytes (IELs) and LP lymphocytes (LPLs) from *Il10*$^{-/-}$ and *Il10*$^{-/-}$*Tlr4*$^{-/-}$ mice were isolated and stimulated with anti-CD3/CD28 Abs. Colonic lymphocytes from *Il10*$^{-/-}$*Tlr4*$^{-/-}$ mice produced significantly higher levels of proinflammatory cytokines such as IL-6, IL-17A, TNF-α, or IFN-γ when compared with colonic lymphocytes from *Il10*$^{-/-}$ mice (Figure 2, B and C).

Table 1
qRT-PCR analysis of RNA samples isolated from colon of mice of the different genotypes

	B6	*Il10*$^{-/-}$	*Il10*$^{-/-}$*Tlr4*$^{-/-}$	*Il10*$^{-/-}$*Tlr9*$^{-/-}$
Cytokines				
IL-6	0.54 ± 0.11	1 ± 0.22	6.33 ± 0.50^{A}	1.49 ± 0.48
Il12p40	0.22 ± 0.16	1 ± 0.18	20.8 ± 1.39^{B}	0.91 ± 0.11
IFN-γ	0.68 ± 0.13	1 ± 0.32	11.8 ± 0.24^{B}	1.88 ± 0.38
IL-1β	0.41 ± 0.21	1 ± 0.14	17.8 ± 0.58^{B}	1.08 ± 0.09
IL-23p19	0.38 ± 0.08	1 ± 0.81	2.11 ± 0.32^{A}	0.43 ± 0.37
TNF-α	0.51 ± 0.38	1 ± 1.03	3.06 ± 0.08^{A}	0.95 ± 0.71
IL-17	0.26 ± 0.31	1 ± 0.08	7.61 ± 0.58^{B}	0.61 ± 0.55
Chemokines				
KC	0.48 ± 0.21	1 ± 0.31	24.1 ± 0.71^{B}	1.11 ± 0.19
MIP1α	0.71 ± 0.13	1 ± 0.08	8.09 ± 0.22^{B}	2.07 ± 0.36
MIP1β	0.57 ± 0.46	1 ± 0.18	13.9 ± 0.28^{B}	1.59 ± 0.52
CCL19	0.59 ± 0.15	1 ± 0.09	7.38 ± 0.39^{B}	1.74 ± 0.74
CXCL10	0.71 ± 0.28	1 ± 0.54	3.73 ± 0.41^{A}	1.03 ± 0.08
CCL22	0.62 ± 0.31	1 ± 0.35	1.95 ± 1.73	1.14 ± 0.48
Cell markers				
F4/80	0.49 ± 0.39	1 ± 0.27	2.52 ± 0.23^{A}	0.91 ± 0.21
MPO	1.01 ± 0.18	1 ± 0.09	10.0 ± 0.39^{B}	1.91 ± 3.16
CD3d	0.75 ± 0.11	1 ± 0.11	13.7 ± 0.38^{B}	2.67 ± 0.24^{A}
CD4	0.68 ± 0.09	1 ± 0.12	3.64 ± 0.28^{A}	1.04 ± 0.08

Results were normalized to those obtained from *Il10*$^{-/-}$ mice, which were designated as 1 unit. Data are expressed as mean ± SD of 6 mice/group. $^{A}P < 0.05$. $^{B}P < 0.01$.

TLR4 expression on effector CD4^{+} *T cells restrains colitis in an adoptive transfer model*. Colitis in *Il10*$^{-/-}$ mice depends on CD4^{+} T cells (3). To determine whether the accelerated colitis observed in *Il10*$^{-/-}$*Tlr4*$^{-/-}$ is dependent on effector CD4^{+} T cells, we carried out 2 different experiments. First, we selectively depleted the CD4^{+} population by injecting anti-CD4 depleting Abs into *Il10*$^{-/-}$*Tlr4*$^{-/-}$ mice (Supplemental Figure 2A). Depletion of CD4^{+} cells resulted 2 weeks later in significant inhibition of crypt hyperplasia, cellular infiltration, and suppression of the colonic proinflammatory cytokine profile (Supplemental Figure 2, B and C). Second, we transferred naive CD4^{+} T cells (i.e., CD4^{+}CD45RB^{hi}) from *Il10*$^{-/-}$ or from *Il10*$^{-/-}$*Tlr4*$^{-/-}$ donor mice to *Rag1*$^{-/-}$ recipients (12) and evaluated the subsequent colitis 8 weeks later. As a control, we cotransferred CD4^{+}CD45RB^{lo}CD25^{+} Tregs from wild-type C57BL/6 (B6) mice along with the naive CD4^{+} subsets from *Il10*$^{-/-}$ or *Il10*$^{-/-}$*Tlr4*$^{-/-}$ mice. We observed that naive CD45RB^{hi} T cells from *Il10*$^{-/-}$*Tlr4*$^{-/-}$ induced greater body weight loss than those from *Il10*$^{-/-}$ mice (Figure 3A). As expected, the cotransfer of CD45RB^{lo}CD25^{+} T cells from B6 mice inhibited the induction of colitis in the recipients (Figure 3B). In accordance with the body weight data, histological analysis of the colonic tissues revealed more severe inflammation in mice that received the naive CD4^{+} T cells from the *Il10*$^{-/-}$*Tlr4*$^{-/-}$ mice. The colitis in these recipients was characterized by depletion of goblet cells and marked abnormalities in the crypt structure, such as crypt hyperplasia, cellular infiltration, and distorted crypt orientation (Figure 3C). Morphometric quantification of the crypt length (Figure 3D) and the number of infiltrating cells (Figure 3E) revealed a significant increase in these inflammatory parameters in mice transferred with naive TLR4-deficient CD4^{+} cells. In some areas, we detected crypt abscesses that were not detected upon transfer of naive CD4^{+} T cells from *Il10*$^{-/-}$ mice (Figure 3C). Furthermore, increased proinflammatory cytokines were generated by CEs taken from recipients transferred with naive CD4^{+} T cells from *Il10*$^{-/-}$*Tlr4*$^{-/-}$ mice as compared with recipients transferred with naive CD4^{+} T cells from *Il10*$^{-/-}$ mice (Figure 3F). We next analyzed the cytokine production by CD4^{+} T cells harvested from different organs of the recipient mice. CD4^{+} T cells from the spleen, MLNs, and colonic mucosa (IELs and LPLs) were isolated and stimulated with anti-CD3/CD28 Abs. While there was no significant difference in the cytokine production by splenic CD4^{+} T cells, we found that MLN CD4^{+} T cells isolated from recipients reconstituted with naive *Il10*$^{-/-}$*Tlr4*$^{-/-}$ cells produced higher levels of IFN-γ. Moreover, the CD4^{+} IELs and LPLs from these recipients produced higher levels of IL-6, IFN-γ, and IL-17A (Figure 3G). Of note, the adoptive transfer of naive *Tlr4*$^{-/-}$ CD4^{+} T cells to *Rag1*$^{-/-}$ recipients also resulted in greater loss of body weight and in more severe colitis than that induced by B6 naive CD4^{+} cells (Supplemental Figure 3). To explore whether the increased inflammatory phenotype observed after adoptive transfer of *Il10*$^{-/-}$*Tlr4*$^{-/-}$ T cells was due to decreased Treg development, we checked the frequency of Foxp3^{+} cells by IHC in colonic tissue from *Rag1*$^{-/-}$ recipients transferred with the indicated CD4^{+} T cell populations. Consistent with previous results (13), the presence of Foxp3^{+} cells was higher in the highly inflamed colons, i.e., the frequency of Foxp3^{+} Tregs arising from the *Il10*$^{-/-}$*Tlr4*$^{-/-}$ CD45RB^{hi} naive population was increased when compared with the number of Foxp3^{+} Tregs observed in the colons of mice receiving *Il10*$^{-/-}$ CD45RB^{hi} cells (Supplemental Figure 4, A and B). Similar numbers of Foxp3^{+} cells were found in the mice receiving Treg cells from B6 mice (cotransfer groups). Collectively, these data suggest that TLR4 ligation exerts a tonic inhibitory effect on colitogenic CD4^{+} T cells.

To further verify this effect, we injected anti-TLR4 blocking Ab to *Il10*$^{-/-}$ mice. The blockade of TLR4 resulted in an increase in the production of proinflammatory cytokines by MLN CD4^{+} T cells after anti-CD3/CD28 Ab stimulation (Supplemental Figure 5A). Similarly, CEs from these mice displayed higher levels of IL-6, IFN-γ, IL-17A, and TNF-α (Supplemental Figure 5B). Taken together, these data demonstrate that the lack of TLR4 on IL-10–deficient CD4^{+} T cells impacts their inflammatory profile.

Naive CD4^{+} *T cells express functional TLR4*. The expression of TLR4 on naive CD4^{+} T cells was recently reported (14, 15). Others groups documented TLR4 expression in Tregs (16) as well as in colitogenic LP CD4^{+} cells (17). Consistent with these reports, we detected TLR4 expression in gated CD3^{+}CD4^{+} cells from spleen of B6 and *Il10*$^{-/-}$ mice (Supplemental Figure 6). As expected, TLR4 expression was absent in the double-deficient *Il10*$^{-/-}$*Tlr4*$^{-/-}$ mice (Supplemental Figure 6). Our finding that TLR4-deficient effector CD4^{+} T cells display different inflammatory phenotypes at various sites (Figure 3, F and G) led us to hypothesize that TLR4 expression on these cells may be the result of a site-specific or an activation-induced regulation. We therefore analyzed the level of TLR4 expression in FACS-sorted CD4^{+} T cells isolated from spleen and MLN of *Il10*$^{-/-}$ mice by quantitative RT-PCR (qPCR). The purity of the analyzed CD4^{+} populations was greater than 99% (data not shown). First, we observed different levels of TLR4 expression in CD4^{+} T cells isolated from different organs (Figure 4A), and the lowest expression was observed in LPLs and IELs. Second, and consistent with a previous report (15), we observed that the expression of TLR4 in these cells was downregulated by TCR stimulation (Figure 4B).

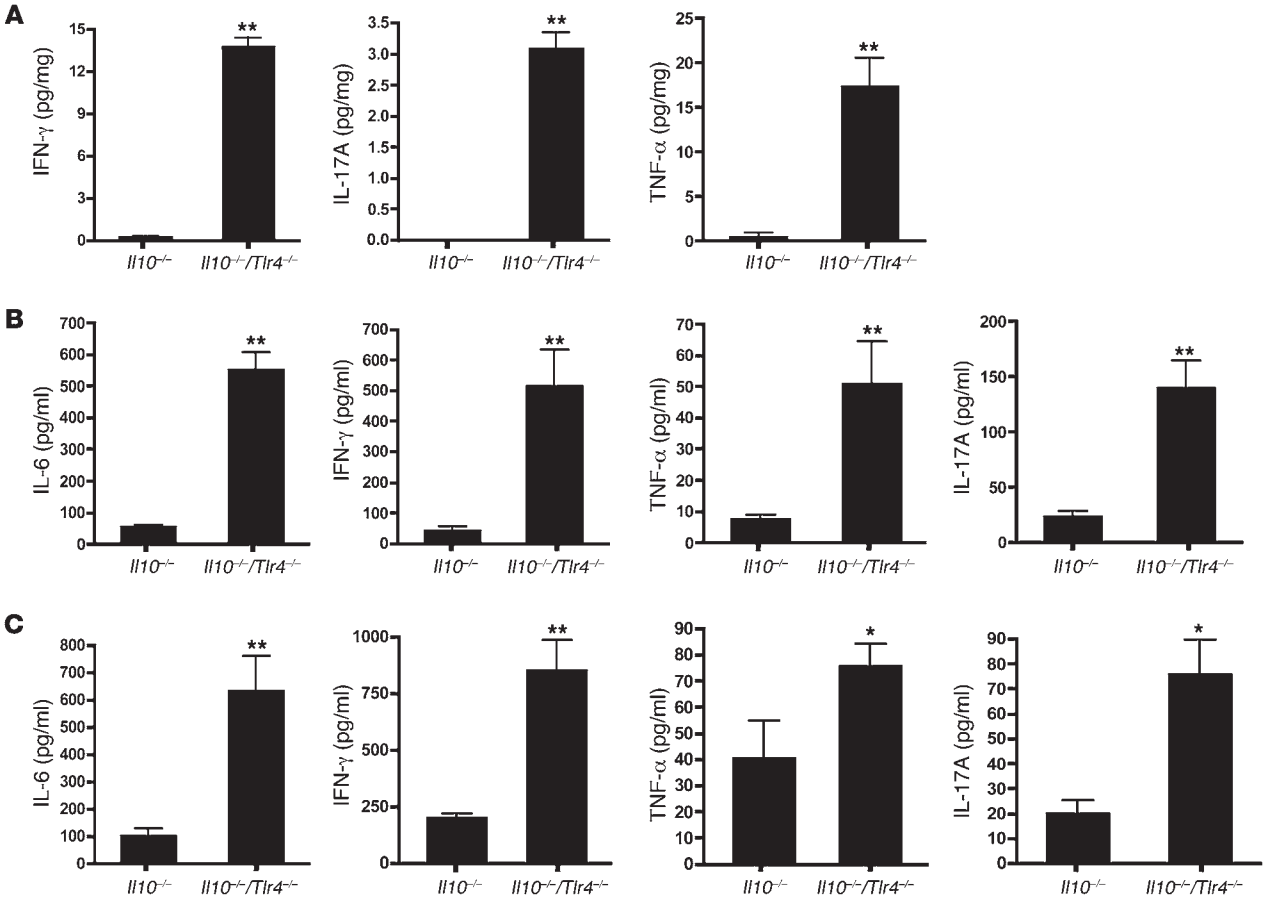

Figure 2

Il10$^{-/-}$*Tlr4*$^{-/-}$ mice develop an increased colonic proinflammatory profile. (**A**) Cytokine levels in CE supernatants after 24 hours of culture (ELISA). Represented values are normalized to milligrams of cultured colonic tissue. (**B** and **C**) Cytokine levels obtained from LPLs (**B**) and IELs (**C**) isolated from the colons of *Il10*$^{-/-}$ and *Il10*$^{-/-}$*Tlr4*$^{-/-}$ mice and stimulated with anti-CD3/CD28 Abs for 24 hours Data represent mean ± SEM of 3 different experiments. **P* < 0.05, ***P* < 0.01.

Since TLR4 deficiency in effector CD4$^+$ T cells affected their inflammatory phenotype in vivo, we explored TLR4 signaling in CD4$^+$ T cells. LPS stimulation led to the activation of the NF-κB signaling pathway (Figure 4C), as well as to the phosphorylation of members of the MAPK family, i.e., p38, JNK, and ERK1/2 (Figure 4D). As expected, MLN-derived CD4$^+$ T cells from *Tlr4*$^{-/-}$ mice were unresponsive to LPS stimulation (Figure 4, E and F).

TLR4 signaling downregulates IFN-γ production through ERK1/2 inhibition. As LPS is a soluble mediator, its interaction with its receptor (TLR4) on CD4$^+$ T cells is not restricted to lymphoid organs. This is in contrast to the cognate TCR-MHCII complex interaction of T cells with APCs. We therefore reasoned that at intestinal mucosal sites, there is a considerable chance of having TLR4-stimulated CD4$^+$ T cells prior to their TCR engagement. To further explore the impact of LPS signaling on CD4$^+$ T cell function, splenic CD4$^+$ T cells from OVA-transgenic (OT-II) mice were prestimulated with LPS, or left unstimulated, before being cocultured with OVA-loaded bone marrow dendritic cells (BMDCs; wild-type) for 5 days. Interestingly, LPS pretreatment significantly reduced the production of IFN-γ by CD4$^+$ T cells while increasing the production of IL-17A (Figure 5A). The levels of other cytokines, such as TNF-α or IL-2, remained unaffected by LPS pretreatment followed by TCR stimulation (data not shown). Similar data were observed in the BMDC-free system, in which CD4$^+$ T cells from B6 mice (spleen, MLN, and colonic LP) were stimulated with LPS followed by anti-CD3/CD28 Abs (Supplemental Figure 7, A and B).

To delineate the signaling mechanism by which LPS exerts its regulatory effect on subsequent TCR activation, we isolated FACS-sorted MLN CD4$^+$ T cells from *Il10*$^{-/-}$ mice and incubated them in the presence or absence of LPS for 2 hours and then stimulated them with anti-CD3/CD28 Abs. LPS stimulation alone induced the translocation of NF-κB (Figure 5B). However, LPS pretreatment had no significant effect on the TCR-dependent NF-κB translocation compared with that observed after TCR activation alone (Figure 5B). In contrast, phosphorylation of MAPK family members was strongly affected by the LPS pretreatment. Specifically, TLR4 triggering prior to TCR stimulation strongly inhibited p-ERK1/2 levels, whereas p-p38 levels were only slightly affected by LPS pretreatment (Figure 5C). Similarly, using intracellular staining (FACS), we detected a 3-fold difference in geometric mean fluorescence (GMF) intensity of p-ERK1/2 after 2 hours of LPS pretreatment (Figure 5D). A similar trend of p-ERK1/2 inhibition was also observed for lower concentrations of LPS (Supplemental Figure 8, A and B). Activation of nuclear factor of activated

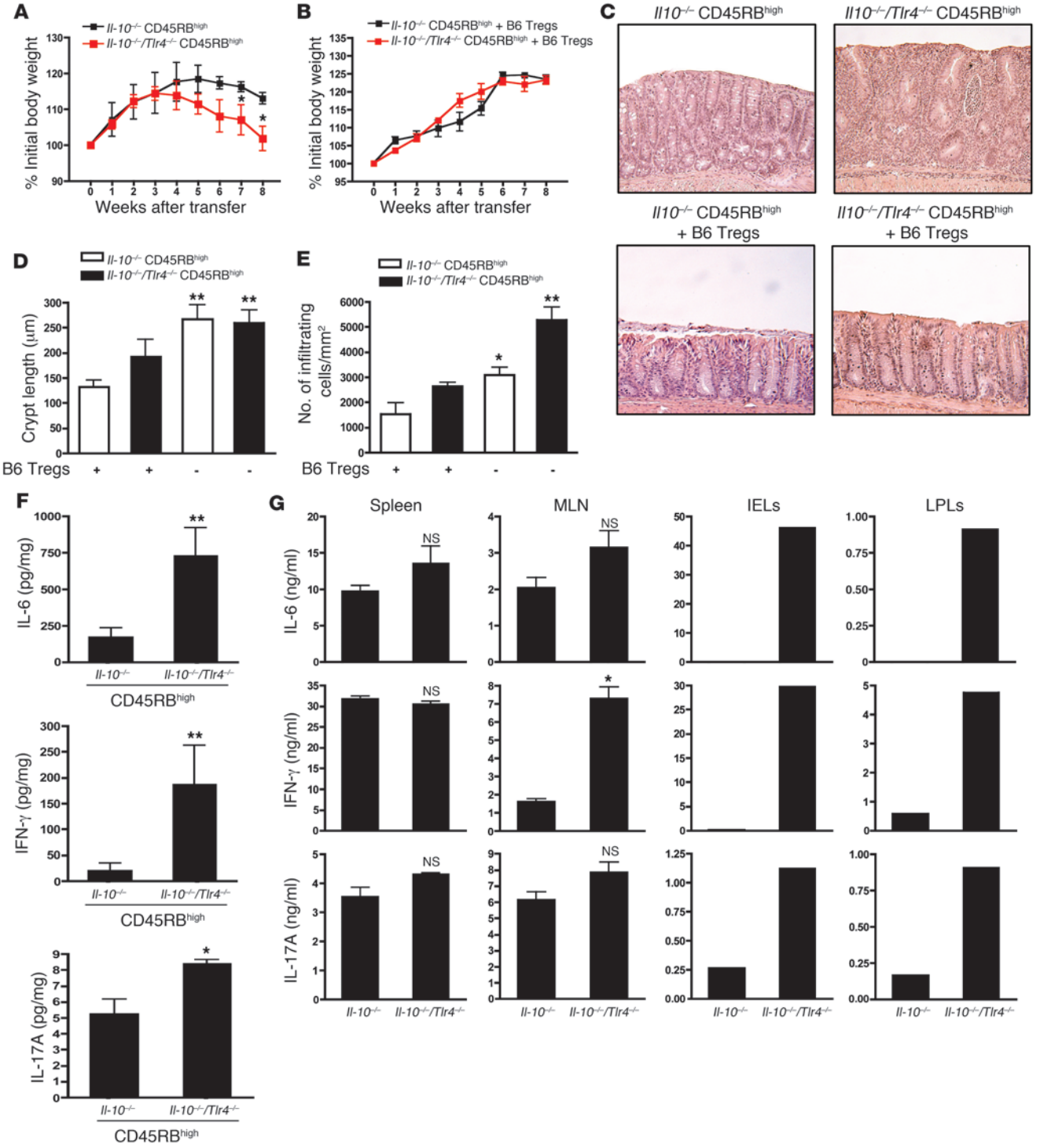

Figure 3

TLR4 expression on CD4+ T cells restrains colitis in an adoptive transfer model. (**A** and **B**) Percentage of initial body weight of *Rag1*$^{-/-}$ recipients transferred with *Il10*$^{-/-}$ and *Il10*$^{-/-}$*Tlr4*$^{-/-}$ FACS-sorted naive CD45RB^{hi} T cells (**A**) and cotransferred with regulatory CD45RB^{lo}CD25^{+} Tregs (B6) (**B**). (**C**) Microscopic evaluation revealed mild inflammation in the colons of *Il10*$^{-/-}$ CD45RB^{hi} recipients, while severe inflammation was observed in the colon of *Il10*$^{-/-}$*Tlr4*$^{-/-}$ CD45RB^{hi} recipients (original magnification, ×100). (**D** and **E**) Quantitative analyses of crypt length and cellular infiltration performed in colonic tissues from the recipient mice. Asterisks represent significant differences compared with control group (group receiving *Il10*$^{-/-}$ naive and B6 Tregs). (**F**) Cytokine levels in CE supernatants after 24 hours of culture. (**G**) CD4+ T cell cytokine response. CD4+ cells from colon (IELs and LPLs), MLNs, and spleen were isolated from *Rag1*$^{-/-}$ recipients and stimulated with anti-CD3/CD28 Abs. Cytokine levels were determined 24 hours later. Data represent mean ± SEM of 2 independent experiments. *$P < 0.05$, **$P < 0.01$.

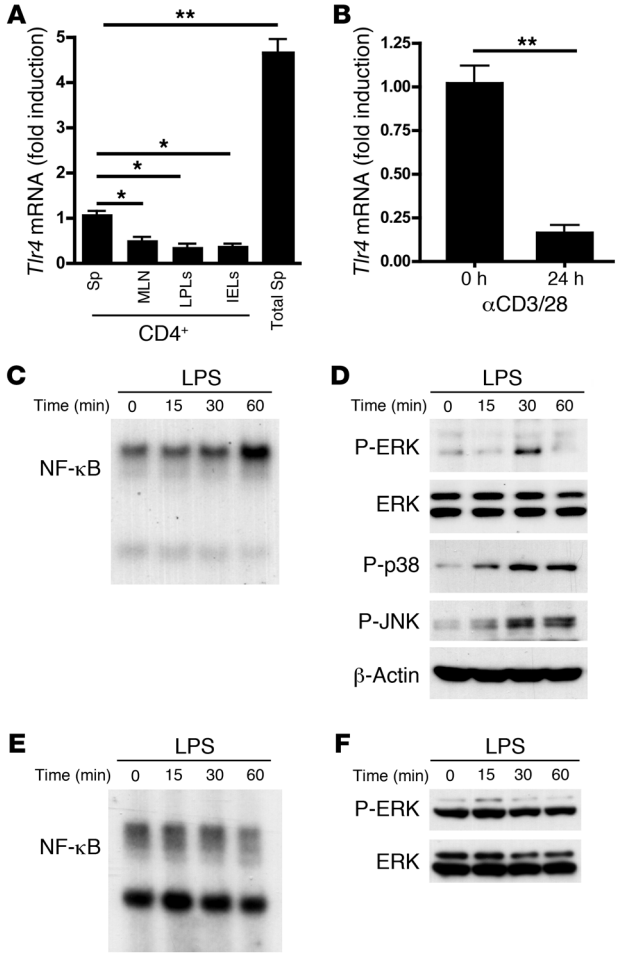

Figure 4
CD4+ T cells express functional TLR4. (**A**) qPCR analysis of *Tlr4* expression in unstimulated CD4+ T cells from spleens (Sp), MLNs, LPLs, and IELs of *Il10*$^{-/-}$ mice. Total splenocytes (Total Sp) were used as a positive control. (**B**) qPCR analysis of *Tlr4* expression in spleen CD4+ T cells before and 24 hours after anti-CD3/CD28 Abs stimulation. (**C** and **D**) MLN CD4+ T cells were treated with LPS for the indicated times. Nuclear lysates were examined for NF-κB activation (EMSA) (**C**), and cytosolic lysates were tested for ERK1/2, p38, and JNK activation by immunoblotting with phospho-specific Abs (**D**). (**E** and **F**) NF-κB and ERK activation in *Tlr4*$^{-/-}$ MLN CD4+ T cells after LPS stimulation. All CD4+ T cells used were FACS sorted, and purity was greater than 98% in all experiments. Stimulation was carried out with 100 ng/ml of LPS in all experiments. Data represent mean ± SEM and are representative of 3 independent experiments (4 mice per experiment were used in **A** and **B**). *$P < 0.05$, **$P < 0.01$.

T cells–1 (NFAT-1) was unaffected by LPS pretreatment (Figure 5E). Of note, costimulation of TLR4 and TCR did not have the same inhibitory impact on either the activation of ERK1/2 or the production of IFN-γ (Supplemental Figure 9).

Since pretreatment with LPS resulted in a significant reduction in IFN-γ production (Figure 5A) and inhibition of ERK1/2 phosphorylation (Figure 5C) in CD4+ T cells, we asked whether these findings are linked. To explore this issue, we pretreated the CD4+ T cells with the specific MEK1/2 inhibitor UO126 before TCR stimulation with anti-CD3/CDCD28 Abs. Similarly to LPS pretreatment, UO126 pretreatment reduced the mRNA expression level of IFN-γ (Figure 5F), while the transcript levels of other proinflammatory cytokines such as IL-6 and IL-17A were not significantly altered by MEK/ERK inhibition (data not shown).

TLR4 signaling regulates subsequent TCR signaling events via the induction of MAPK phosphatases. The lack of ERK1/2 activation induced by LPS treatment of CD4+ T cells could be explained by either diminished phosphorylation by MEK1/2 or increased dephosphorylation of p-ERK1/2 by specific phosphatases. As shown in Supplemental Figure 10, LPS pretreatment did not inhibit the TCR-dependent phosphorylation of MEK1/2, indicating that inhibition of p-ERK1/2 is not due to an upstream event. MAPK enzymes undergo inactivation by MAPK phosphatases (MKPs), also known as dual-specificity protein phosphatases (DUSPs), which dephosphorylate both phosphothreonine and phosphotyrosine residues on activated MAPKs (18). Since the expression of several MKPs was documented in T cells (19–21), we tested whether TLR4 triggering regulates p-ERK1/2 through the induction of MKPs. Indeed, we found that LPS stimulation of *Il10*$^{-/-}$ CD4+ T cells led to a marked increase in cytosolic MKP-3 (Figure 6A). In accordance with these data, freshly isolated MLN CD4+ T cells from *Il10*$^{-/-}$*Tlr4*$^{-/-}$ mice showed reduced expression of MKP-3 (Figure 6B). Moreover, LPS pretreatment led to increased levels of both nuclear MKP-1 and cytosolic MKP-3 upon subsequent anti-CD3/CD28 Abs stimulation (Figure 6C). In contrast, TCR activation alone did not induce any activation of MKP-1 or MKP-3 in these cells at the tested time period (Figure 6C). The phosphorylation level of SHIP-1, a phosphatase that is associated with LPS tolerance in macrophages (22), was largely unaffected by LPS stimulation of *Il10*$^{-/-}$ CD4+ T cells or in *Il10*$^{-/-}$*Tlr4*$^{-/-}$ mice (Figure 6, A and B). In contrast, a slight increase in the TCR-dependent phosphorylation of SHIP-1 was observed after LPS pretreatment (Figure 6C).

As MKP-3 was downregulated in *Il10*$^{-/-}$*Tlr4*$^{-/-}$ CD4+ T cells (Figure 6B), and since it was shown to specifically regulate ERK1/2 while minimally affecting other MAPKs (23), we next explored its impact on *Il10*$^{-/-}$ CD4+ T cell activation profile by gene silencing (Figure 6D). MKP-3 knockdown abrogated the LPS-dependent downregulation of ERK1/2 activation in vitro, as determined by FACS-based intracellular staining (Figure 6E). LPS pretreatment resulted in a marked decrease in both the percentage of p-ERK1/2–positive cells and the GMF intensity in the control siRNA transfected cells, whereas such an effect was not observed in MKP-3 siRNA transfected cells (Figure 6E). MKP-3 knockdown also abrogated the LPS-dependent downregulation of IFN-γ production by anti-CD3/CD28 Abs stimulation but did not affect IL-17A production (Figure 6F).

TLR4 signals through 2 adaptors, MyD88 and TRIF. To further explore the mechanism by which TLR4 exerts its control over MKP-3 activation, we examined whether this effect is dependent on the MyD88- or the TRIF-mediated signaling. We stimulated MLN-derived CD4+ T cells from *Il10*$^{-/-}$*Myd88*$^{-/-}$ or *Il10*$^{-/-}$/LPS2 mice (the LPS2 mouse has a *Trif*$^{-/-}$ phenotype) (24) with LPS and checked the subsequent MKP-3 activation. Interestingly, MKP-3 activation was unaffected in the absence of MyD88 but was strongly reduced in LPS2 CD4+ T cells (Supplemental Figure 11). These data indicate that TLR4 activates MKP-3 in a TRIF-dependent manner and provide a possible explanation for the different phenotypes observed in *Il10*$^{-/-}$*Tlr4*$^{-/-}$ and *Il10*$^{-/-}$*Tlr9*$^{-/-}$ mice (Figure 1, A and B).

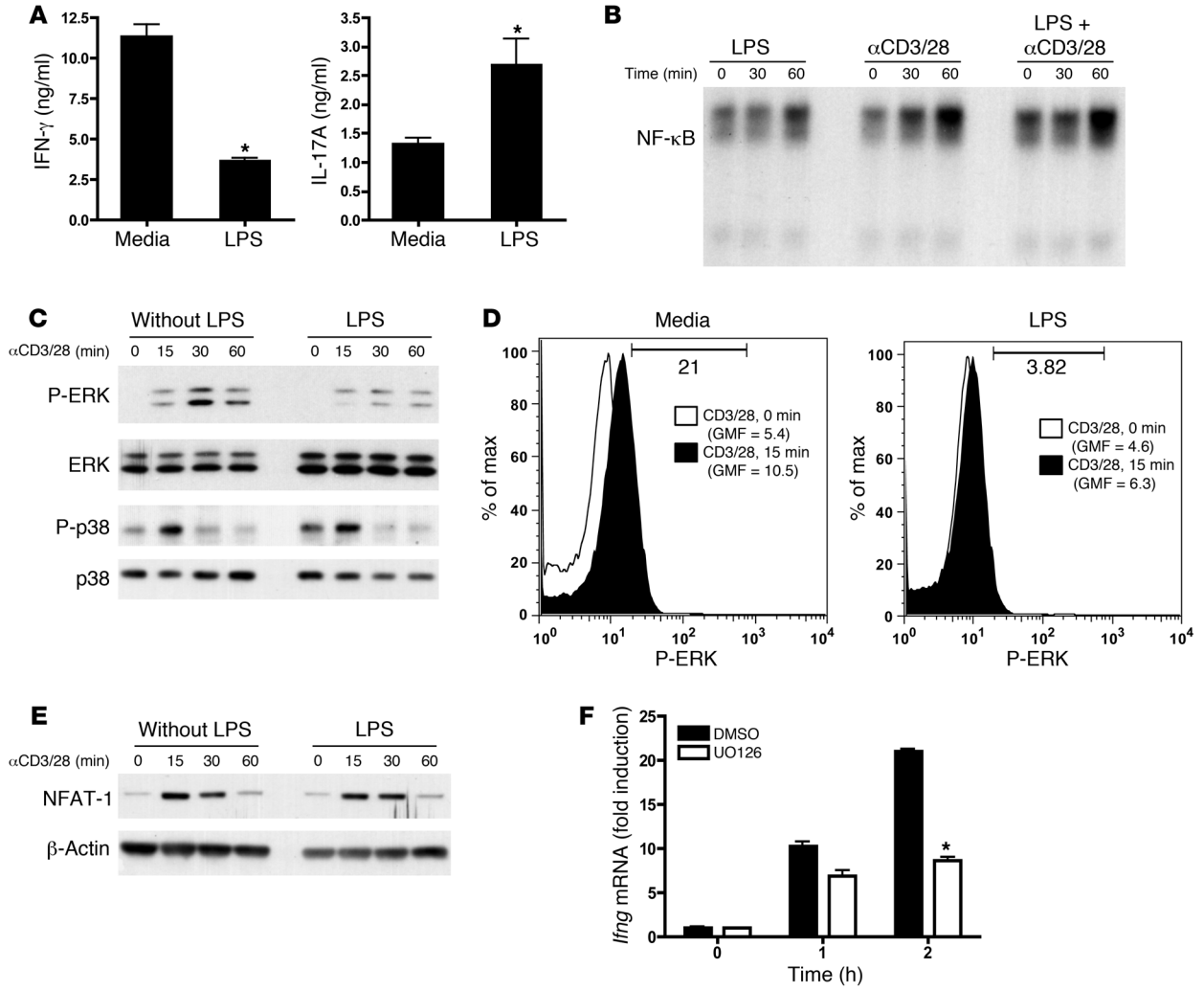

Figure 5

TLR4 signaling in CD4+ T cells downregulates IFN-γ production through ERK1/2 inhibition. (**A**) Splenic CD4+ T cells from OT-II mice were incubated for 2 hours in the presence of 100 ng/ml LPS or medium alone. The cells were then washed and cultured for 5 days with OVA-loaded BMDCs. After coculture, the CD4+ cells were restimulated, and the secretion of cytokines was determined 24 hours later. (**B**) NF-κB activation was assessed in nuclear extracts by EMSA. (**C**) Cytosolic lysates were immunoblotted for MAPK protein activation after anti-CD3/CD28 Ab stimulation with or without LPS (100 ng/ml) for 2 hours prior to TCR stimulation. (**D**) LPS-dependent regulation of ERK1/2 phosphorylation was confirmed by phospho-protein analysis by flow cytometry as described in Methods. Numbers within histograms denote the percentage of p-ERK1/2–positive cells in stimulated cells when compared with control cells. (**E**) Activation of NFAT-1 was measured by immunoblotting of nuclear extracts from CD4+ cells stimulated as in **C**. (**F**) RT-PCR analysis of CD4+ T cells incubated with the MEK/ERK1/2 inhibitor UO126 or vehicle (DMSO) before being stimulated with anti-CD3/CD28 Abs for the indicated times. Data in **A**–**F** represent mean ± SEM of 3 independent experiments. *$P < 0.05$. All experiments, except in **A**, were carried out with FACS-sorted MLN-derived CD4+ cells from *Il10*$^{-/-}$ mice (purity, >98%).

To validate that the increased inflammation observed in the absence of TLR4 signaling in the *Il10*$^{-/-}$ mice is related to the lack of induction of MKPs, we inhibited MKPs in vivo using a cell-permeable, quinone-based inhibitor of dual-specificity phosphatases, NSC 95397, which inhibits both MKP-1 and MKP-3 (25). Injection of a single dose of this compound into *Il10*$^{-/-}$ mice resulted 3 days later in significant body weight loss and diarrhea as compared with vehicle-treated mice (Supplemental Figure 12, A and B). Furthermore, the number of CD4+ T cells present in MLNs of mice treated with NSC 95397 was also increased when compared with vehicle-treated mice (Supplemental Figure 12C). In addition to these signs of intestinal inflammation, the administration of this compound in vivo resulted in the upregulated expression of p-ERK1/2 in freshly isolated MLN-derived CD4+ T cells (Figure 6G). More importantly, stimulation of these MLN CD4+ T cells with anti-CD3/CD28 Abs resulted in increased production of proinflammatory cytokines (Figure 6H). Finally, in vivo blockade of TLR4 signaling in *Il10*$^{-/-}$ mice by administration of anti-TLR4 blocking Abs led to a reduction in the basal expression of MKP-1 and MKP-3 in freshly isolated CD4+ T cells from spleen and MLN (Supplemental Figure 13). In addition, as discussed above, in vivo blockade of TLR4 led to increased production of proinflammatory cytokines by stimulated MLN CD4+ T cells and by CEs (Supplemental Figure 5, A and B). However, no changes in body weight or

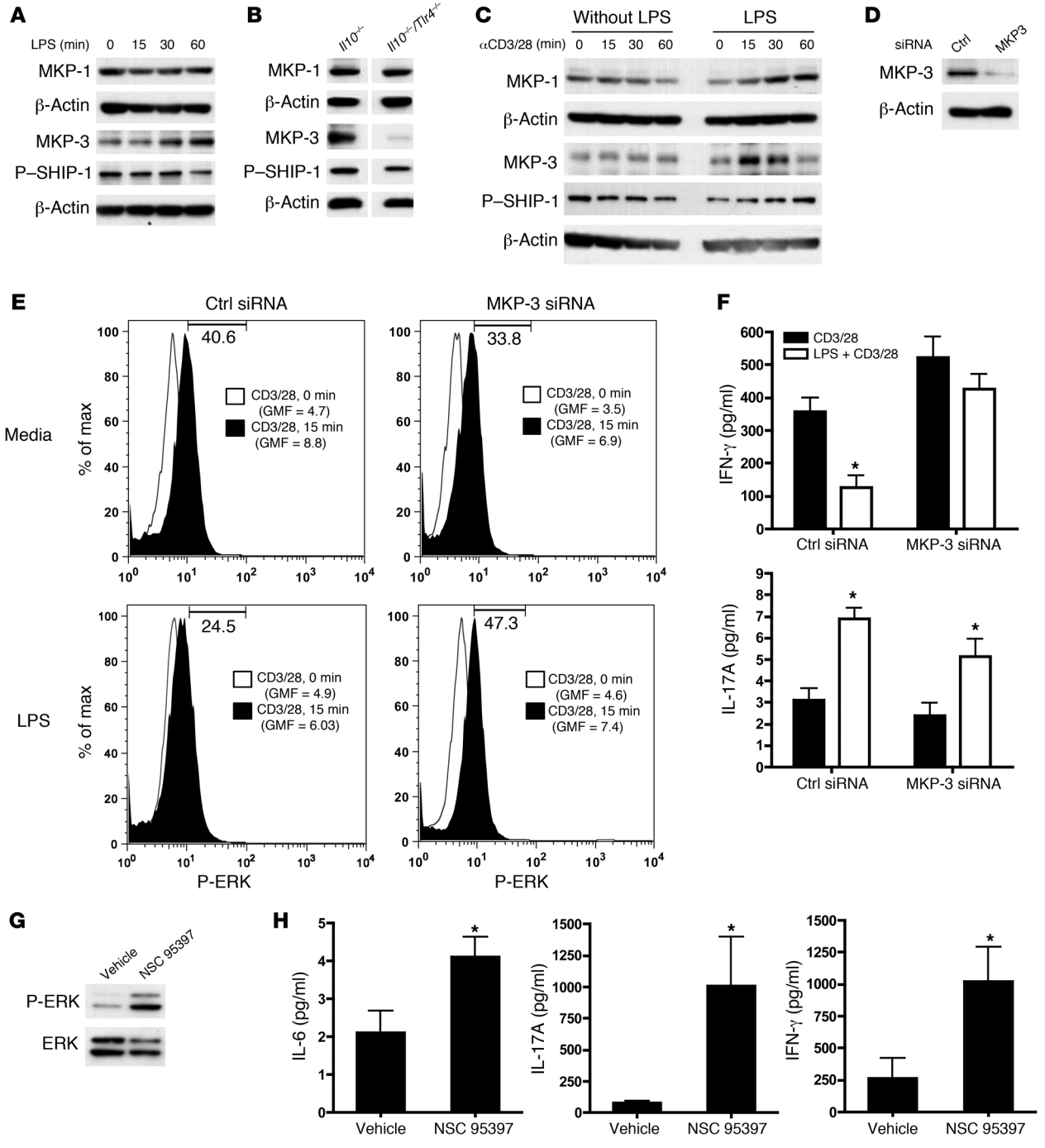

Figure 6

TLR4 modulates TCR-dependent MAPK phosphatase activation. (**A**) Immunoblot analysis of the indicated phosphatases after LPS stimulation of CD4+ cells at different time points. (**B**) Expression of MKPs and p-SHIP1 in freshly isolated, unstimulated CD4+ cells from *Il10*$^{-/-}$ and *Il10*$^{-/-}$*Tlr4*$^{-/-}$ mice. (**C**) Immunoblotting of protein extracts from CD4+ T cells stimulated with LPS or left untreated before stimulation with anti-CD3/28 Abs for different periods of time. (**D**) Analysis of the siRNA knockdown in CD4+ T cells 24 hours after transfection with either MKP-3 or control siRNA (Ctrl). (**E**) TCR-dependent phosphorylation of ERK1/2 24 hours after transfection with MKP-3 or control siRNA. Numbers within histograms denote percentage of p-ERK1/2–positive cells in stimulated cells when compared with control cells. (**F**) Cytokine levels measured from 24-hour supernatants of cells treated as in **E**. Data represent mean ± SEM. (**G**) p-ERK expression in freshly isolated CD4+ cells from *Il10*$^{-/-}$ mice treated with MKP inhibitor in vivo (NSC 95397) or vehicle. (**H**) Cytokine levels after 24 hours of anti-CD3/28 Ab stimulation of MLN-derived CD4+ T cells isolated from *Il10*$^{-/-}$ mice 3 days after injection of NSC 95397 or vehicle. Data represent mean ± SEM. Data are representative of at least 2 independent experiments. *$P < 0.05$. All experiments were carried out with FACS-sorted MLN-derived CD4+ cells from *Il10*$^{-/-}$ or *Il10*$^{-/-}$*Tlr4*$^{-/-}$ mice (purity, >98%). Stimulation was carried out with 100 ng/ml LPS in all experiments. The lanes shown in **B** were run on the same gel but were noncontiguous.

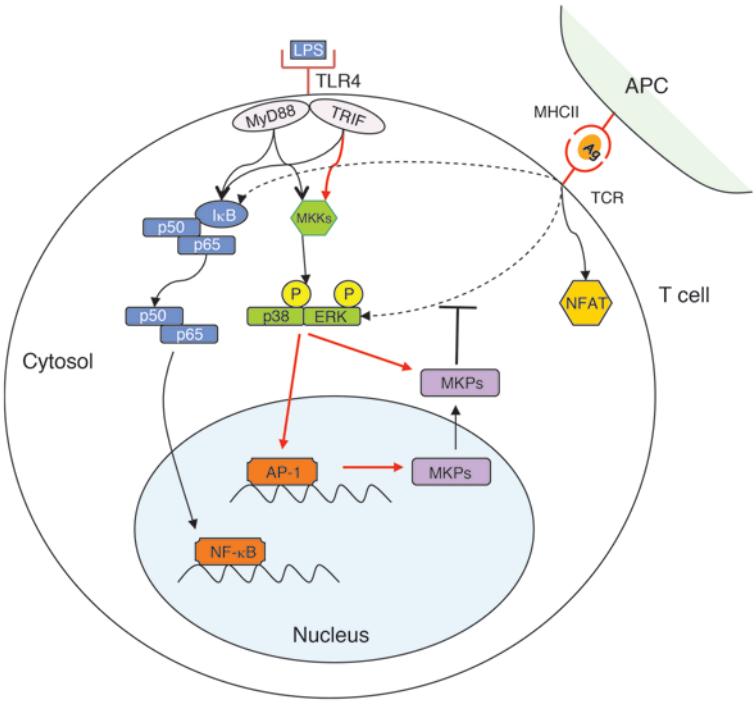

Figure 7
Proposed mechanism of TLR4-dependent regulation of TCR activation (conditional activation). TLR4 triggering of CD4+ T cells activates NF-κB and MAPK pathways. However, the induction of MKP1 and MKP3 occurs mainly via the TRIF pathway. The high levels of MKP-1 and MKP-3 restrain a subsequent TCR-dependent activation of p38 and ERK, respectively. This activation of phosphatases in CD4+ T cells by TLR4 restrains subsequent TCR-induced phosphorylation events and, hence, modulates CD4+ T cell responses and their inflammatory phenotypes. AP-1, activator protein 1; MKK, MAPK kinase.

histological score (crypt elongation and infiltration) were observed in mice treated with TLR4 blocking antibody. Repeated treatment and/or longer follow-up may be required to identify colonic inflammation induced by TLR4 blockade.

Collectively, these data indicate that TLR4 signaling in colitogenic CD4+ T cells regulate their activation mainly through the induction of MKP-3 that restrains p-ERK levels upon subsequent TCR stimulation (Figure 7).

Discussion

TLR activation of APCs (i.e., dendritic cells or macrophages) by their signature microbial ligands, leads to the induction of an inflammatory program that enhances APC maturation (26). The mature APC provokes CD4+ T cell activation, proliferation, and differentiation (26, 27). Recent evidence and this study indicate that certain TLRs are also expressed in CD4+ T cells, suggesting that their ligands may affect T cell functions (10, 14–17).

Vivarium conditions affect the age at which colitis develops and the severity of colitis in *Il10*$^{-/-}$ mice (28). While signs of colitis were barely detectable in 8-month-old *Il10*$^{-/-}$ or *Il10*$^{-/-}$*Tlr9*$^{-/-}$ mice, we could easily identify severe colitis in 8-week-old *Il10*$^{-/-}$*Tlr4*$^{-/-}$ mice (Figures 1 and 2, Table 1, and Supplemental Figure 1). Although the TLR4 deficiency in innate immune cells contributes to colitis severity (9, 29), the impact of its deficiency in effector CD4+ T cells, in these models, has not been investigated. To further explore the latter, we adoptively transferred naive *Il10*$^{-/-}$*Tlr4*$^{-/-}$ CD4+ T cells into IL-10–sufficient and TLR4-sufficient *Rag1*$^{-/-}$ recipients. The transfer of these CD4+ T cells produced higher levels of proinflammatory cytokines and induced more aggressive colitis as compared with that in recipients transferred with naive *Il10*$^{-/-}$ CD4+ T cells (Figure 3).

The colitis observed in *Il10*$^{-/-}$ mice was originally described as a Th1-mediated inflammation, which could be ameliorated by neutralizing Abs to IL-12p40 and IFN-γ (2, 30). Recently, Th17 cells were shown to inflict the colonic immunopathology in these mice (31). It is most likely that these 2 inflammatory cytokines contribute to the development of colitis at different stages. IFN-γ is required for the initiation, whereas IL-17 is required for the perpetuation of colitis, as was documented recently (32).

At the molecular level, pretreatment of CD4+ T cells with LPS decreased ERK1/2 phosphorylation upon TCR stimulation (Figure 5). This effect can be attributed, largely, to the induction of certain MKPs, in particular MKP-3. The induced MKP-3 dephosphorylated p-ERK1/2 and therefore restrained the subsequent intensity of TCR signaling and, hence, cytokine production. The different kinetics in the induction of MKP-1 and -3 levels by LPS or by LPS followed by TCR stimulation (Figure 6, A and C) may suggest the involvement of transcriptional and posttranslational events. Indeed, ERK1/2 activation was shown recently to play a key role in *MKP3* gene transcription (33) and in posttranslational modification necessary for MKP-1 activation (34–36). MKPs are highly regulated under inflammatory conditions. Indeed, glucocorticoids or IL-10 induce MKP-1 expression (37–39), while IFN-γ attenuates it and therefore enhances MAPK activation (40). Our data also indicate the important role of TLR4 signaling in the induction of MKP-1 and -3 in CD4+ T cells, especially at intestinal mucosal sites. Taken together, these observations explain why the combined deficiency of IL-10 and TLR4 in *Il10*$^{-/-}$*Tlr4*$^{-/-}$ mice makes these animals so susceptible to the development of aggressive colitis at an early age.

Interestingly, in our study and others (41, 42), certain aspects of the cytokine profile induced by LPS in TLR4-sufficient CD4+ T cells in vitro (Figure 5A) did not fully correlate with the pattern seen in vivo. Specifically, we found IL-17A levels to be increased after LPS and anti-CD3/CD28 stimulation in vitro, whereas *Il10*$^{-/-}$*Tlr4*$^{-/-}$ mice had increased IL-17A levels compared with *Il10*$^{-/-}$ mice (Figure 2, Figure 3, and Table 1). This discrepancy may be explained by the different conditions involved in CD4+ T cell activation in vivo (e.g., different TCR-MHCII interactions, the involvement of costimula-

tory molecules other than CD28, and the co-triggering of CD4+ T cells by other TLR agonists) compared with those we used in vitro. Of note, both in vitro and in vivo data indicate the inhibition of IFN-γ production by CD4+ T cells after LPS pretreatment.

The role of the adaptor protein MyD88 in commensal-dependent colitis in *Il10*$^{-/-}$ mice was recently addressed (43). In that study, the genetic co-deletion of MyD88 completely abolished the induction of colitis, CD4+ T cell activation, and Th1 phenotype differentiation in the LP. Our data indicate that the results obtained with *Il10*$^{-/-}$*Myd88*$^{-/-}$ cannot be extrapolated to all TLR-deficient *Il10*$^{-/-}$ mice, as different MyD88-dependent TLRs have different impacts on the activation profile of innate immune cells and adaptive immune cells, as was demonstrated in this study. This TLR-dependent differential activation of innate versus adaptive cells regulates the phenotype of colitis in the *Il10*$^{-/-}$ host (Figures 1 and 2).

A recent publication addressed the role of Treg function in the absence of IL-10 and TLR4 signals (i.e., *Il10*$^{-/-}$*Tlr4*$^{-/-}$ mice) in a model of intestinal inflammation mediated by *Helicobacter hepaticus* (13). In accordance with our data, the authors reported an increase in intestinal inflammation in *Il10*$^{-/-}$*Tlr4*$^{-/-}$ mice with enhanced production of Th1/Th17 cytokines from effector CD4+ T cells, accompanied by an increase in IFN-γ–producing Foxp3+ Treg cells. Thus, TLR4 signaling enhances the regulatory function of Tregs (13) and, as presented in this study, inhibits the inflammatory function of activated effector CD4+ T cells. It is therefore most likely that these 2 different effects of TLR4 synergize in the regulation of intestinal inflammation.

In summary, our results demonstrate that LPS stimulation modulates the subsequent TCR signaling and the subsequent inflammatory phenotype of the related effector CD4+ T cells, independent of the expression of this receptor in innate immune cells. Both TLR and TCR signaling pathways utilize members of the MAPK family. As presented above, TLR activation of these pathways influences the subsequent TCR-mediated signaling events and CD4+ T cell function. In this respect, our findings expand the current meaning of "LPS tolerance" to include the restraining effects of LPS on CD4+ T cell function. These data underline the importance of what we term conditional activation of CD4+ T cells. Here, CD4+ T cells are triggered by cytokine or other innate immune receptors that use certain signaling pathways/molecules shared by TCR. The impact of conditional activation on the cytokine and proliferative T cell responses can be determined and appreciated only after a subsequent TCR activation (Figure 7). This mechanism therefore explains the dissimilar activation profile of CD4+ T cells isolated from different organs observed in this (Figure 3G) and other studies and underlines the physiological role of conditional activation in the regulation of T cell responses.

Methods

Mice. Six- to 10-week-old mice were used for all the experimental procedures. Specific pathogen–free B6 mice were purchased from Harlan. *Rag1*$^{-/-}$ and *Il10*$^{-/-}$ mice on the B6 background were originally purchased from The Jackson Laboratory and maintained under specific pathogen–free conditions in our vivarium. *Tlr4*$^{-/-}$, *Tlr2*$^{-/-}$, *Tlr9*$^{-/-}$, and *Myd88*$^{-/-}$ mice were provided by S. Akira (Osaka University, Osaka, Japan), and LPS2 mice (B6) were provided by B. Beutler (The Scripps Research Institute, San Diego, California, USA). All mice were bred in our vivarium. All TLR-deficient strains were backcrossed onto the B6 background for 10 generations. To generate the double-KO mice (e.g., *Il10*$^{-/-}$*Tlr4*$^{-/-}$), *Il10*$^{-/-}$ mice were intercrossed with the different *Tlr*$^{-/-}$ related mice. All experimental procedures were approved by the IACUC of UCSD. Transgenic OT-II mice were purchased from The Jackson Laboratory.

Reagents. LPS from *Salmonella minnesota* Re595 was prepared and used as described previously (44, 45). Chicken OVA and the MKP inhibitor NSC 95397 were purchased from Sigma-Aldrich. The specific ERK inhibitor UO126 was purchased from Promega.

Culture and stimulation of CD4+ cells. Complete RPMI 1640 (Irvine Scientific) medium supplemented with 10% heat-inactivated FCS, 2 mM L-glutamine, 100 U/ml penicillin, and 100 μg/ml streptomycin was used throughout the experiments. Spleen- and MLN-derived CD4+ T cells were negatively selected by using the CD4+ Isolation Kit (Miltenyi Biotec). The enriched CD4+ population was then stained with anti-CD3 and anti-CD4 monoclonal Abs (both from eBioscience) and FACS-sorted with a MoFlow Cytometer equipped with Summit Software (Dako). Purity of the enriched populations was greater than 99% in all the experiments. After sorting, CD4+ T cells were cultured in complete RPMI medium and stimulated with 5 μg/ml plate-bound anti-CD3 and 1 μg/ml anti-CD28 Abs. Twenty-four hours culture supernatants were collected for cytokine analysis using ELISA (eBioscience). For the signaling experiments, FACS-sorted CD4+ T cells were pre-stimulated with 100 ng/ml of LPS for 2 hours or left untreated, before stimulation with 5 μg/ml anti-CD3 and 1 μg/ml anti-CD28 Abs for the indicated time points.

Splenic CD4+ T cells from TCR transgenic mice specific for OVA (OT-II) were isolated as described above. BMDCs were cultured and harvested as previously described (46, 47). BMDCs were loaded with 2 μg/ml of I-A^{d}–restricted OVA peptide (OVA$_{323-339}$: ISQAVHAAHAEINEAGR, PeptidoGenic Research) 2 hours before the addition of OT-II CD4+ cells to the culture. After 5 days of coculture, CD4+ T cells were recovered and restimulated with anti-CD3 and anti-CD28 Abs for 24 hours. Supernatants were then collected and cytokines levels measured by ELISA.

For the inhibition of ERK1/2 phosphorylation, splenic CD4+ T cells from *Il10*$^{-/-}$ mice were incubated for 30 minutes with 10 μM UO126 or vehicle (DMSO), before the stimulation with anti-CD3/CD28 Abs. Cells were then collected at different times, and their RNA was isolated and subjected to quantitative RT-PCR analysis.

Evaluation of colitis. The entire colon was excised, opened longitudinally, rolled onto a wooden stick, fixed with Bouin's solution, and embedded in paraffin. Five-micrometer tissue sections were prepared, deparaffinized, and stained with H&E. Colons were analyzed for 2 parameters, crypt length and inflammatory cell infiltration. Crypt lengths were measured on 2 representative photographs of each colon, and means of the 2 longest crypts were calculated. Inflammatory cell infiltration into the LP was evaluated on a representative high-magnification photograph of each colon by manual counting. The resulting cell counts were related to the area of the image and are expressed as numbers of infiltrating cells per mm^2 tissue.

Isolation of RNA and quantitative RT-PCR. The isolation of RNA was carried out using an RNeasy Mini Kit (QIAGEN) according to the manufacturer's instructions. After isolation, RNA was treated with DNase I (Invitrogen) to digest contaminating DNA. One microgram of RNA sample was then used for reverse transcription and synthesis of cDNA using Superscript III First-Strand system (Invitrogen). Quantitative real-time PCR was performed on an AB7300 (Applied Biosystems) using SYBR Green PCR Master Mix (Applied Biosystems). GAPDH expression was used as internal reference in all PCR experiments. RT-PCR primers (Supplemental Table 1) for specific target genes were designed based on their reported sequences and synthesized by IDT Technologies.

Culture of CEs. Cytokine levels in the cultured media of CEs were measured by ELISA as previously described (48). Briefly, 3- to 4-cm colonic samples were weighed and washed in RPMI 1640 medium containing 100 μg/ml streptomycin and 100 U/ml penicillin. The CEs were cultured for 24 hours in complete RPMI 1640 at 37°C and 5% CO_2. Culture super-

natants were then collected and cytokine levels measured using sandwich ELISAs for IL-6, TNF-α, IFN-γ, and IL-17A (eBioscience).

Induction of colitis by adoptive transfer of CD45RB^{hi} CD4$^+$ T cells. Splenocytes from *Il10*$^{-/-}$, *Il10*$^{-/-}$*Tlr4*$^{-/-}$, and B6 donor mice were enriched for CD4$^+$ T cells using immunomagnetic bead separation as described above. Cells were stained with PE-Cy5–anti-CD4 (L3T4) (eBioscience), PE–anti-CD25 (PC61), and FITC–anti-CD45RB (16A) (BD Biosciences — Pharmingen) and sorted into naive CD4$^+$CD45RB^{hi} and regulatory CD4$^+$CD45RB^{lo}CD25$^+$ populations (purity, >98%) with a MoFlow Flow Cytometer (Dako) using Summit software. Seven- to 9-week-old RAG1-deficient mice were used as recipients. To eliminate the risk of infection by pathogens in the recipients, we added to the food an antibiotic cocktail containing amoxicillin (0.6 mg/g food), clarithromycin (0.1 mg/g food), metronidazole (0.2 mg/g food), and omeprazole (0.004 mg/g food) (Bio-Serv) for 2 weeks before the T cell transfer. After antibiotic treatment, sex-matched mice were transplanted by i.p injection with 5×10^5 CD45RB^{hi} naive T cells from *Il10*$^{-/-}$ or *Il10*$^{-/-}$*Tlr4*$^{-/-}$ mice. For the cotransfer experiments, 2×10^5 CD45RB^{lo}CD25$^+$ Tregs from B6 mice were coinjected with the naive CD4$^+$ T cell population. After reconstitution, mice were monitored for signs of intestinal inflammation such as weight loss and diarrhea. Diseased animals were sacrificed for analysis between 8 and 10 weeks after transfer. Crypt length and infiltration of cells into the LP were determined as described above.

Isolation of LPLs and IELs. Isolation of LPLs and IELs was performed as described previously (49). Briefly, colons were washed with PBS and cut into 1-cm pieces. The intestinal pieces were incubated with HBSS/5 mM EDTA/1 mM DTT solution for 20 minutes at 37°C under rotation. After this predigestion step, the pieces were filtered through a 100-μm cell strainer, and the flow-through containing IELs was collected in a fresh tube. The predigestion step was repeated to ensure maximum recovery of IELs. After washing off the remaining EDTA with fresh PBS, the tissue was cut into smaller pieces (~1–2 mm) and digested with 1× PBS containing 0.5 mg/ml collagenase D (Roche), 0.5 mg/ml DNase I (Sigma-Aldrich), and 3 mg/ml Dispase II (Roche) 3 times, 20 minutes each, at 37°C under rotation. After digestion, LPLs were collected using a 40-μm cell strainer. Finally, the IELs and LPLs were isolated by centrifugation with 40/80 Percoll (Sigma-Aldrich) gradient for 20 minutes at 1,000 *g* at 20°C without braking. IELs and LPLs were cultured in complete RPMI 1640 medium and stimulated with anti-CD3/CDCD28 Abs as described above.

EMSA and immunoblotting. Translocation of activated NF-κB into the nucleus was measured by EMSA using consensus NF-κB oligonucleotides (Santa Cruz Biotechnology Inc.) as previously described (44). For immunoblotting, the following antibodies were used: anti–p-SHIP1, anti–p-ERK, anti–p-p38, anti–p-JNK, anti-p38, and anti-ERK (Cell Signaling Technology); anti-IκBα, anti–MKP-1, and anti–MKP-3 (Santa Cruz Biotechnology Inc.); anti–NFAT-1 (Abcam); and anti–β-actin (Sigma-Aldrich).

Gene silencing by siRNA. Purified CD4$^+$ T cells from MLNs were transfected by electroporation using a mouse T cell Nucleofector kit (Amaxa), according to the manufacturer's protocol. Briefly, CD4$^+$ cells were resuspended in mouse T cell nucleofection solution at a density of 2×10^6 to 3×10^6 cells per 100 μl. For each transfection, 100 μl of cell suspension was mixed with 500 nM of either control siRNA or MKP-3 siRNA (Santa Cruz Biotechnology Inc.) (mRNA accession: NM_026268; strand 1, GAAGGUGGCUUCAGUAAGU; strand 2, GAACGAUGCUUACGACAUU; strand 3, GGACAUCCAUCCAGAUAGA). Cells were then transferred into a cuvette and pulsed in a Nucleofector II device. After electroporation, cells were collected and incubated in pre-equilibrated mouse T cell nucleofector medium at 37°C and 5% CO_2. Stimulation of the CD4$^+$ cells was carried out 24 hours after transfection.

Phospho-protein analysis by flow cytometry. Intracellular p-ERK1/2 staining was carried out as previously described (50). In brief, MLN-derived CD4$^+$ cells were either left unstimulated or stimulated with LPS for 2 hours. After LPS prestimulation, cells were challenged with anti-CD3/CDCD28 Abs as described above. After stimulation, cells were fixed in 1.5% paraformaldehyde/PBS for 10 minutes at room temperature. Cells were then centrifuged and permeabilized in 100% methanol for 20 minutes at 4°C or overnight at –20°C. After permeabilization, cells were washed with FACS buffer (PBS/5% BSA/0.2% NaN_3) and stained with anti-CD4 Ab (Clone GK1.5) (eBioscience) and anti–p-ERK1/2 Ab (Clone 20a) (BD Biosciences) for 30 minutes at room temperature and in the dark. Cells were finally washed and analyzed in a BD FACSCalibur flow cytometer (BD Biosciences).

In vivo inhibition of MAPK phosphatases. *Il10*$^{-/-}$ mice aged 6–7 weeks were injected i.p with a single dose of 4 mg/kg body weight of the MKP inhibitor NSC 95397 (Sigma-Aldrich) in 200 μl of a PBS/2.5% DMSO vehicle solution. As a control, a group of mice received 200 μl of the vehicle solution alone. Mice were monitored every day and sacrificed at day 3 after the injection. MLN-derived CD4$^+$ cells were isolated and stimulated as described above.

Administration of anti-TLR4 neutralizing antibody. Blockade of TLR4 in *Il10*$^{-/-}$ mice was carried out by i.p. administration of 100 μg of anti-mouse TLR4/MD2 antibody clone MTS510 (eBioscience) every week for a total of 2 weeks. Rat IgG2a isotype control clone eBR2a (100 μg; eBioscience) was injected into the control mice. Mice were monitored for signs of inflammation twice a week and sacrificed 2 weeks after the beginning of the treatment. CD4$^+$ cells from spleen and MLN were isolated and stimulated as described above.

Statistics. Values are displayed as mean ± SEM or mean ± SD as indicated. Statistical differences between groups were analyzed using the nonparametric Mann-Whitney *U* test for quantitative data. All *P* values are 2-tailed, and *P* values less than 0.05 were considered significant. All calculations were performed using Prism 4.0 software.

Acknowledgments

We thank Scott Herdman and Lucinda Beck for critical review of the manuscript. This work was supported by NIH grants AI68685, DK35108, DK080506, and CA133702 and a grant from the Crohn's and Colitis Foundation of America (CCFA).

Received for publication June 2, 2009, and accepted in revised form November 11, 2009.

Address correspondence to: José M. González-Navajas or Eyal Raz, Department of Medicine, University of California, San Diego, 9500 Gilman Drive, La Jolla, California 92093, USA. Phone: (858) 534-5380; Fax: (858) 534-0409; E-mail: jog001@ucsd.edu (J.M. González-Navajas). Phone: (858) 534-5444; Fax: (858) 534-0409; E-mail: eraz@ucsd.edu (E. Raz).

1. Groux H, et al. A CD4+ T-cell subset inhibits antigen-specific T-cell responses and prevents colitis. *Nature*. 1997;389(6652):737–742.
2. Kuhn R, Lohler J, Rennick D, Rajewsky K, Muller W. Interleukin-10-deficient mice develop chronic enterocolitis. *Cell*. 1993;75(2):263–274.
3. Roers A, et al. T cell-specific inactivation of the interleukin 10 gene in mice results in enhanced T cell responses but normal innate responses to lipopolysaccharide or skin irritation. *J Exp Med*. 2004;200(10):1289–1297.
4. Kim SC, et al. Variable phenotypes of enterocolitis in interleukin 10-deficient mice monoassociated with two different commensal bacteria. *Gastroenterology*. 2005;128(4):891–906.
5. Madsen KL. Inflammatory bowel disease: lessons from the IL-10 gene-deficient mouse. *Clin Invest Med*. 2001;24(5):250–257.
6. Akira S, Hemmi H. Recognition of pathogen-associated molecular patterns by TLR family. *Immunol Lett*. 2003;85(2):85–95.
7. Katakura K, Lee J, Rachmilewitz D, Li G, Eckmann L, Raz E. Toll-like receptor 9-induced type I IFN protects mice from experimental colitis. *J Clin Invest*. 2005;115(3):695–702.
8. Rachmilewitz D, et al Immunostimulatory DNA ameliorates experimental and spontaneous murine

colitis. *Gastroenterology*. 2002;122(5):1428–1441.
9. Rakoff-Nahoum S, Paglino J, Eslami-Varzaneh F, Edberg S, Medzhitov R. Recognition of commensal microflora by toll-like receptors is required for intestinal homeostasis. *Cell*. 2004;118(2):229–241.
10. Kabelitz D. Expression and function of Toll-like receptors in T lymphocytes. *Curr Opin Immunol*. 2007;19(1):39–45.
11. Ivanov II, et al. Specific microbiota direct the differentiation of IL-17-producing T-helper cells in the mucosa of the small intestine. *Cell Host Microbe*. 2008;4(4):337–349.
12. Powrie F, Leach MW, Mauze S, Caddle LB, Coffman RL. Phenotypically distinct subsets of CD4+ T cells induce or protect from chronic intestinal inflammation in C. B-17 scid mice. *Int Immunol*. 1993; 5(11):1461–1471.
13. Matharu KS, et al. Toll-like receptor 4-mediated regulation of spontaneous Helicobacter-dependent colitis in il-10-deficient mice. *Gastroenterology*. 2009; 137(4):1380–1390.e3.
14. Fukata M, et al. The myeloid differentiation factor 88 (MyD88) is required for CD4+ T cell effector function in a murine model of inflammatory bowel disease. *J Immunol*. 2008;180(3):1886–1894.
15. Gelman AE, Zhang J, Choi Y, Turka LA. Toll-like receptor ligands directly promote activated CD4+ T cell survival. *J Immunol*. 2004;172(10):6065–6073.
16. Caramalho I, Lopes-Carvalho T, Ostler D, Zelenay S, Haury M, Demengeot J. Regulatory T cells selectively express toll-like receptors and are activated by lipopolysaccharide. *J Exp Med*. 2003;197(4):403–411.
17. Tomita T, et al. MyD88-Dependent pathway in T cells directly modulates the expansion of colitogenic CD4+ T cells in chronic colitis. *J Immunol*. 2008; 180(8):5291–5299.
18. Liu Y, Shepherd EG, Nelin LD. MAPK phosphatases — regulating the immune response. *Nat Rev Immunol*. 2007;7(3):202–212.
19. Jeffrey KL, et al. Positive regulation of immune cell function and inflammatory responses by phosphatase PAC-1. *Nat Immunol*. 2006;7(3):274–283.
20. Kurt RA, Urba WJ, Smith JW, Schoof DD. Peripheral T lymphocytes from women with breast cancer exhibit abnormal protein expression of several signaling molecules. *Int J Cancer*. 1998;78(1):16–20.
21. Zhang Y, et al. Regulation of innate and adaptive immune responses by MAP kinase phosphatase 5. *Nature*. 2004;430(7001):793–797.
22. Sly LM, Rauh MJ, Kalesnikoff J, Song CH, Krystal G. LPS-induced upregulation of SHIP is essential for endotoxin tolerance. *Immunity*. 2004;21(2):227–239.
23. Maillet M, Purcell NH, Sargent MA, York AJ, Bueno OF, Molkentin JD. DUSP6 (MKP3) null mice show enhanced ERK1/2 phosphorylation at baseline and increased myocyte proliferation in the heart affecting disease susceptibility. *J Biol Chem*. 2008; 283(45):31246–31255.
24. Hoebe K, et al. Identification of Lps2 as a key transducer of MyD88-independent TIR signalling. *Nature*. 2003;424(6950):743–748.
25. Vogt A, McDonald PR, Tamewitz A, Sikorski RP, Wipf P, Skoko JJ III, Lazo JS. A cell-active inhibitor of mitogen-activated protein kinase phosphatases restores paclitaxel-induced apoptosis in dexamethasone-protected cancer cells. *Mol Cancer Ther*. 2008; 7(2):330–340.
26. Iwasaki A, Medzhitov R. Toll-like receptor control of the adaptive immune responses. *Nat Immunol*. 2004;5(10):987–995.
27. Napolitani G, Rinaldi A, Bertoni F, Sallusto F, Lanzavecchia A. Selected Toll-like receptor agonist combinations synergistically trigger a T helper type 1-polarizing program in dendritic cells. *Nat Immunol*. 2005;6(8):769–776.
28. Strauch UG, et al. Influence of intestinal bacteria on induction of regulatory T cells: lessons from a transfer model of colitis. *Gut*. 2005;54(11):1546–1552.
29. Fukata M, et al. Toll-like receptor-4 is required for intestinal response to epithelial injury and limiting bacterial translocation in a murine model of acute colitis. *Am J Physiol Gastrointest Liver Physiol*. 2005;288(5):G1055–G1065.
30. Berg DJ, et al. Enterocolitis and colon cancer in interleukin-10-deficient mice are associated with aberrant cytokine production and CD4(+) TH1-like responses. *J Clin Invest*. 1996;98(4):1010–1020.
31. Yen D, et al. IL-23 is essential for T cell-mediated colitis and promotes inflammation via IL-17 and IL-6. *J Clin Invest*. 2006;116(5):1310–1316.
32. Montufar-Solis D, Schaefer J, Hicks MJ, Klein JR. Massive but selective cytokine dysregulation in the colon of IL-10–/– mice revealed by multiplex analysis. *Int Immunol*. 2008;20(1):141–154.
33. Ekerot M, et al. Negative-feedback regulation of FGF signalling by DUSP6/MKP-3 is driven by ERK1/2 and mediated by Ets factor binding to a conserved site within the DUSP6/MKP-3 gene promoter. *Biochem J*. 2008;412(2):287–298.
34. Brondello JM, Pouyssegur J, McKenzie FR. Reduced MAP kinase phosphatase-1 degradation after p42/p44MAPK-dependent phosphorylation. *Science*. 1999;286(5449):2514–2517.
35. Lin YW, Chuang SM, Yang JL. ERK1/2 achieves sustained activation by stimulating MAPK phosphatase-1 degradation via the ubiquitin-proteasome pathway. *J Biol Chem*. 2003;278(24):21534–21541.
36. Lin YW, Yang JL. Cooperation of ERK and SCF-Skp2 for MKP-1 destruction provides a positive feedback regulation of proliferating signaling. *J Biol Chem*. 2006;281(2):915–926.
37. Abraham SM, et al. Antiinflammatory effects of dexamethasone are partly dependent on induction of dual specificity phosphatase 1. *J Exp Med*. 2006; 203(8):1883–1889.
38. Hammer M, et al. Control of dual-specificity phosphatase-1 expression in activated macrophages by IL-10. *Eur J Immunol*. 2005;35(10):2991–3001.
39. Xiao YQ, et al. Cross-talk between ERK and p38 MAPK mediates selective suppression of pro-inflammatory cytokines by transforming growth factor-beta. *J Biol Chem*. 2002;277(17):14884–14893.
40. Zhao Q, et al. MAP kinase phosphatase 1 controls innate immune responses and suppresses endotoxic shock. *J Exp Med*. 2006;203(1):131–140.
41. Kattah MG, Wong MT, Yocum MD, Utz PJ. Cytokines secreted in response to Toll-like receptor ligand stimulation modulate differentiation of human Th17 cells. *Arthritis Rheum*. 2008;58(6):1619–1629.
42. Kimura A, Naka T, Kishimoto T. IL-6-dependent and -independent pathways in the development of interleukin 17-producing T helper cells. *Proc Natl Acad Sci U S A*. 2007;104(29):12099–12104.
43. Rakoff-Nahoum S, Hao L, Medzhitov R. Role of toll-like receptors in spontaneous commensal-dependent colitis. *Immunity*. 2006;25(2):319–329.
44. Lee J, Mira-Arbibe L, Ulevitch RJ. TAK1 regulates multiple protein kinase cascades activated by bacterial lipopolysaccharide. *J Leukoc Biol*. 2000; 68(6):909–915.
45. Lee J, et al. Molecular basis for the immunostimulatory activity of guanine nucleoside analogs: activation of Toll-like receptor 7. *Proc Natl Acad Sci U S A*. 2003;100(11):6646–6651.
46. Datta SK, et al. A subset of Toll-like receptor ligands induces cross-presentation by bone marrow-derived dendritic cells. *J Immunol*. 2003;170(8):4102–4110.
47. Lutz MB, et al. An advanced culture method for generating large quantities of highly pure dendritic cells from mouse bone marrow. *J Immunol Methods*. 1999;223(1):77–92.
48. Hue S, et al. Interleukin-23 drives innate and T cell-mediated intestinal inflammation. *J Exp Med*. 2006;203(11):2473–2483.
49. Weigmann B, Tubbe I, Seidel D, Nicolaev A, Becker C, Neurath MF. Isolation and subsequent analysis of murine lamina propria mononuclear cells from colonic tissue. *Nat Protoc*. 2007;2(10):2307–2311.
50. Krutzik PO, Nolan GP. Intracellular phospho-protein staining techniques for flow cytometry: monitoring single cell signaling events. *Cytometry A*. 2003;55(2):61–70.